

Algorithms and Accuracy of Transforming Orthophoto Maps into Quadtree Tiling for Google Maps

Sebastian Castillo-Carrion

Virtual Learning and Technological Laboratories,
University of Malaga, Malaga, Spain
E-mail: scastillo@gmail.com

Ruth Romero Jiménez and Jose-Emilio Guerrero-Ginel

Animal Production, University of Cordoba, Cordoba, Spain

Jose-Emilio Meroño-Larriva

Cartography Engineering, Geodesy and Photogrammetry,
University of Cordoba, Cordoba, Spain

Abstract. One of the most important features of a tourist mapping service is its ability to speed up the process of large image navigation. To achieve this goal, most techniques use interactive compressions such as Multiresolution Seamless Image Database, ERMMapper compressed wavelet, and JPEG2000. An alternative approach is proposed in this article using quadtree structures, which allows direct access to information and avoids compression and decompression operations. The proposed strategy is designed to function within a framework of interoperability and integration with the universal search platforms of mapping services. In this study, a photogrammetric image of the entire Andalusia region is used to assess a strategy of cutting and merging images and evaluate the geometric accuracy of the raster data. The proposed approach is shown to result in errors of less than 2.5 m at more than 90% of the control points. © 2012 Society for Imaging Science and Technology. [DOI: 10.2352/J.ImagingSci.Technol.2012.56.1.010502]

INTRODUCTION

The amount of information generated by various disciplines is constantly increasing, leading to difficulties in its management and processing. The growth in the quantity of data needing to be transmitted and stored has given rise to significant advances in the development of new transmission and storage technologies aimed at improving data management and processing. Fiber-optic technology, for example, allows much faster data transmission, while Blu-ray disc permits large amounts of data to be stored in a small physical environment.¹

While it is true that both storage and transmission capacities are steadily increasing, the need for mass storage and transmission still seems to increase at least twice as fast as storage and transmission capacities. There are also situations in which capacity has not increased significantly. For

example, the amount of information we can transmit over the airwaves will always be limited by the characteristics of the atmosphere.² For situations where capacity limitations are difficult to overcome, data compression becomes an attractive option.

The aim of data compression is to reduce redundancy in stored and communicated data, thus increasing effective data density. One benefit of compressing the data to be stored or transmitted is to reduce storage and/or communication costs.³ Two categories of compression algorithms or techniques are currently in use. *Lossless compression* involves no loss of information. The original data can be recovered accurately from the compressed data. This technique is generally used for applications that cannot tolerate any difference between original and reconstructed data, e.g., a compressed text file or program. *Lossy compression* involves loss of information; generally speaking, data that have been compressed using lossy techniques cannot be recovered or reconstructed exactly. In many applications, this lack of exact reconstruction is not a problem, e.g., image (jpg) or video compression (mpg).

Data can be compressed using different techniques, depending on the type of data to be processed.⁴ Geographic information system (GIS) is no exception to this need to compress data. The amount of information being managed is continually growing due to increasing demands from education, land use, environment, urban planning, and land registry. Raster images/orthophotos used in GIS tend to be of higher resolution and require a considerable amount of memory, which impedes agile handling. There is, thus, a need for different compression approaches for a wide range of georeferencing purposes. Some of the commonly used approaches are summarized below.

ERMMapper compressed wavelet (ECW)⁵ developed by Earth Resource Mapping, uses a system based on wavelet

Received Jul. 29, 2011; accepted for publication Nov. 14, 2011; published online Mar. 16, 2012

1062-3701/2012/56(1)/010502/8/\$20.00.

compression with ratios of 25:1 and multiresolution hierarchical data structures that allow quick access to any part of the image. It automatically decompresses the portion of the image with the level of detail requested and compresses it again with another portion from a conventional format such as JPEG. ECWP, developed by Earth Resource Mapping, is a protocol that works over http. It is similar to ECW and is used in conjunction with the Image Web Server product from Earth Resource Mapping.⁶ Multi-resolution Seamless Image Database (MrSID) by LizardTech⁷ and developed at Los Alamos National Laboratory⁸ also employs a wavelet-based system.⁹ JPEG2000 is another wavelet-based standard and *GeoTIFF* embeds georeferencing data in a TIFF file.

The above mentioned compression techniques involve computation cost, due to the need to decompress and process the region of interest. The present study focuses on a quadtree tiling system, which allows access to data in a simple and convenient way while consuming minimal bandwidth. The following sections describe the proposed algorithm to transform orthophoto maps into a quadtree tiling system and the methodology for estimating the geometric accuracy of the resulting maps.

QUADTREE TILING SYSTEM

The proposed approach is based on storing images using a quadtree-based map coordinate in a hierarchical structure of folders, where part of the map is segmented into tiles at different levels of details (zoom level), see Figure 1. This approach provides visualization of detailed maps with aerial and satellite views in a simple and convenient way. Transmission of high-resolution images requires higher bandwidth. However, high-resolution images are not distinguishable from their low-resolution counterparts when viewed from a distance. The basic idea is to utilize minimum bandwidth for maximum distinguishable resolution. High-resolution images are subdivided into tiles, where only viewable tiles are downloaded as needed. This provides the online browsing capability for very high-resolution 2D images without the cost of downloading the entire full-resolution image to the client.¹⁰

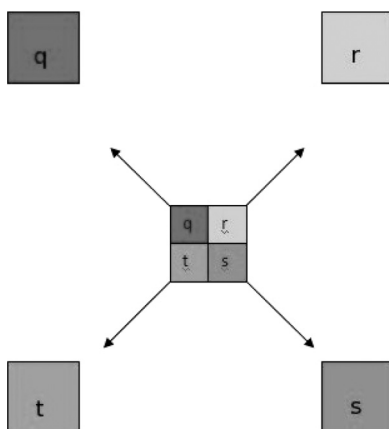


Figure 1. Map cut into tiles with higher resolution.

Since there is no Open Geospatial Consortium specification for a tiled web map service standard, Google developed its own based on a similar tiling scheme with its Google Map service. Google Maps Imagery (Google Maps) makes use of a quadtree system for storing and accessing its pyramid of imagery tiles. It is based on 256-pixel square tiles, compressed in JPG format and organized as “qrst” quadtree-based map coordinates in a hierarchical structure of folders (parts of the map were segmented into tiles at different zoom levels). This is done using the qrst recursive quartered subdivision. The image of the earth is used as tile “t,” level 1 at minimum detail. Divide this into four to get “tq,” “tr,” “ts,” and “tt” (level 2), then divide each of these into four more to get “tqt,” “tqq” (level 3), and so on until the desired N-level of detail is reached,¹¹ see Figure 2. The projection used is the Mercator map projection with system reference WGS84¹² (EPSG 4326). To reach the tile “tqssrrrtqstqssqrsr” (level 18), one starts off at map t and zoom in on tq, obtaining map tq. Subsequently, map tq passes to “tqs,” and so on, until the desired level of detail is reached, as can be seen in Figure 3.

The clever part of the proposed approach is the system used for addressing image tiles, while simultaneously naming and geocoding the files. Each tile is associated with a two-dimensional coordinate system (x, y) in which each coordinate takes values in the interval [0,1]. From the name of a tile, a pair of coordinates can be generated, associated with the upper left corner of the tile. Each coordinate is proportional to the position of the corner in the earth image. For example, Figure 4 shows that the coordinates associated with “qrrs” are (0.4375, 0.0625). Once these coordinates (x, y) have been obtained, its geographical coordinates (22.5° W, 82.6762875814065° N) can be computed using the following equations:¹³

$$\text{Latitude}(y) = 2 \bullet \arctan(e^{((1-2y) \cdot \pi)}) \bullet \frac{180}{\pi} - 90 \quad (1)$$

$$\text{Longitude}(x) = 360 \bullet x - 180 \quad (2)$$

METHODS: SPLITTING, JOINING, AND REPLACEMENT ALGORITHMS

The Andalusia region benefits from the existence of extensively high-quality aerial photography, often much better than that provided by Google. In this article, a three-step algorithm to interface with Google’s massive computing infrastructure is described, which enables the publication of large, raster datasets within the framework of Google Maps.

Preliminary Steps

The Andalusian cartographic database uses European Datum 1950 (ED50) and Universal Transverse Mercator (UTM). It is different from Google, which uses WGS84 and the Mercator projection system. To merge the two dataset, the first step is to transform the Andalusian maps

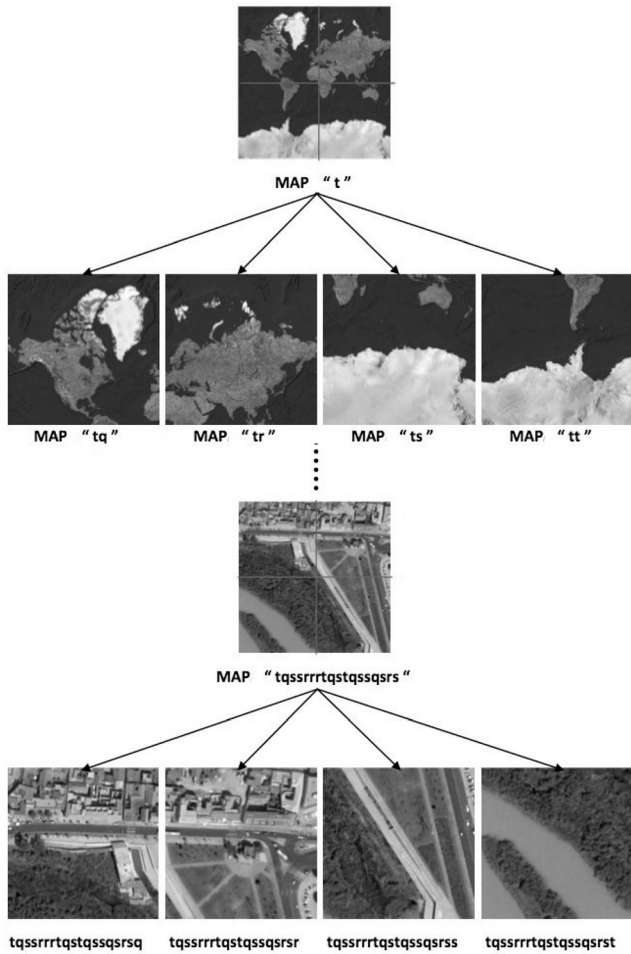


Figure 2. Detailed example of qrst quartered subdivision.

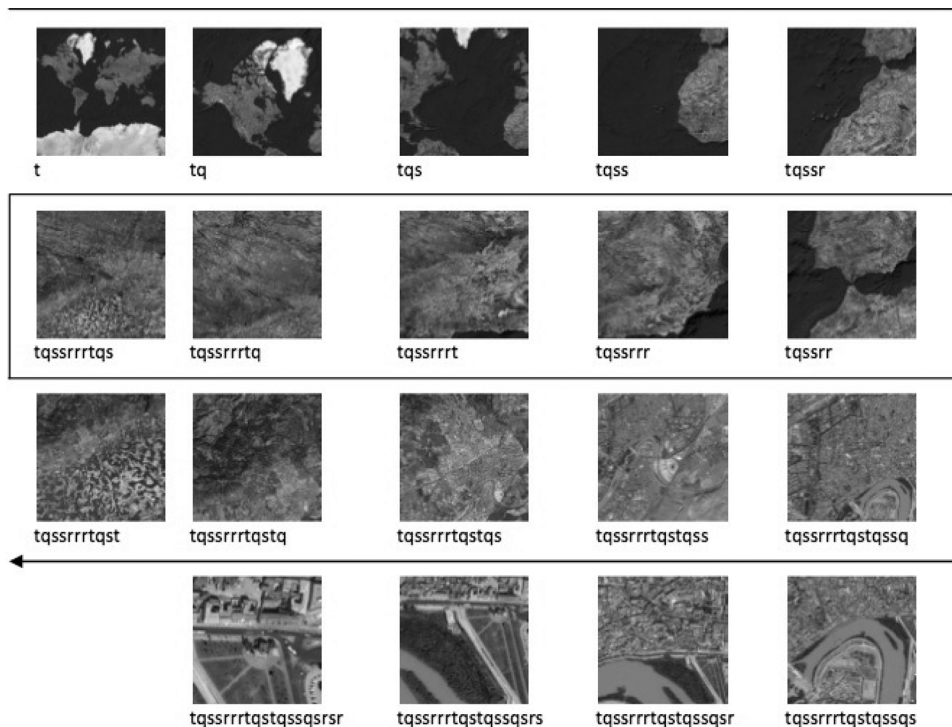


Figure 3. Division of tiles to reach level tqssrrrtqstqssqsr.

to the WGS84 and Mercator projection system, using `orto_pnoa_etr89_vs_ed50`¹⁴ and GDAL utilities.¹⁵ Figure 5 shows the effect of applying this reprojection. Once all the maps have been transformed to WGS84 and reprojected to Mercator, a map database entry was obtained for the subsequent splitting, joining, and replacement algorithms.

Splitting Algorithm

In this step, the algorithm generates all the tile names of the highest required level (level N). For each name, it identifies the area or region and looks for pieces of this area in the map database and creates the tile map through the composition of the pieces obtained. For example, given the name “qssrrrtqstqssqsr,” it identifies the geographical coordinates of its upper left and lower right corners using Eqs. (1) and (2).

Once these two pairs of geographical coordinates have been calculated, the algorithm identifies the maps of the database entry that contains the required area and proceeds to extract the area from those maps. Note that the database entry can be a set of JPEG raster files with georeferential information in plain text format. The extracted images are then used to create a georeferenced tile of 256 × 256 pixels and a JGW plain text file (a file used to georeference a .jpg file, which provides real world coordinate information that allows a corresponding .jpg file to be correctly positioned on a map or in a mapping system) that contains information about the scale of the image per pixel as well as the coordinates of the upper left pixel of this new tile, see Figure 6. If this tile already exists, it will be updated rather than creating a new one. The detail will be discussed in the *Replacement Algorithm* section.

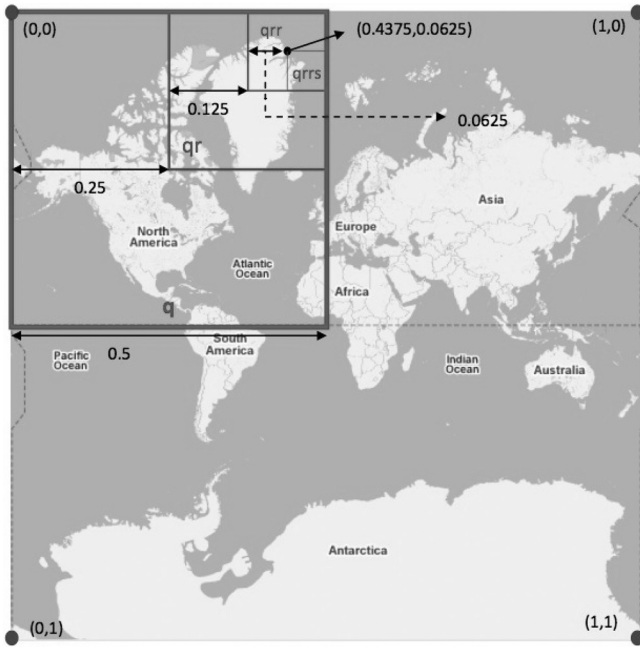


Figure 4. Getting bidimensional coordinates [0, 1] from tile name.

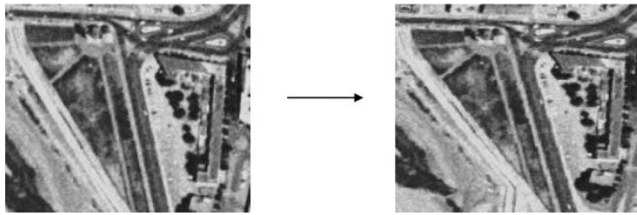


Figure 5. Reproject WGS84 UTM to WGS84 Mercator.

Joining Algorithm

To create a tile at level N-1, its four qrst pyramid subdivision tiles of level N are joined together, and the resulting tile is resized to 256 × 256 pixels. For example, to generate tile “qssrrrtqstqssq,” tiles “qssrrrtqstqssq,” “qssrrrtqstqssqr,” “qssrrrtqstqssqs,” and “qssrrrtqstqssqt” are joined as shown in Figure 7. The joining operation is done using the GDAL utilities. An alternative is to obtain the tile directly from the map database entry at the splitting phase. However, this will require working with image areas too large to be kept in memory, especially when working with lower level tiles, thus consuming more resources and being less efficient.

Replacement Algorithm

No new functionality is introduced added at this step. Replacement simply combines the splitting and joining steps to update tiles with a better map database entry. For example, suppose a better orthophoto database entry is available, which covers only part of the “qssrrrtqstqssq” tile, and it is at the highest level of the pyramid of. Then, part of “qssrrrtqstqssq” is updated with the new region, as shown in Figure 8, during the splitting step. Subsequently, all lower levels are regenerated (updated) via the joining steps, e.g., “qssrrrtqstqss” and “qssrrrtqstqs”.

Results

Splitting and Joining

The objective of the study is to create the tiles form level 8 to 15 of the subpyramid that covers the entire Andalusia region using a set of large Andalusian orthophotos with a 1-m pixel resolution as the map database entry. The goal is to obtain 12 subpyramids of tiles at level 8—qssrrqsq, qssrrqst, qssrrqsr, qssrrqss, qssrrtrr, qssrrrtq, qssrrrtt, qssrrsq, qssrrtrr, qssrrrts, qssrrrsq, qssrrrst—and their seven next levels (see Figure 9).

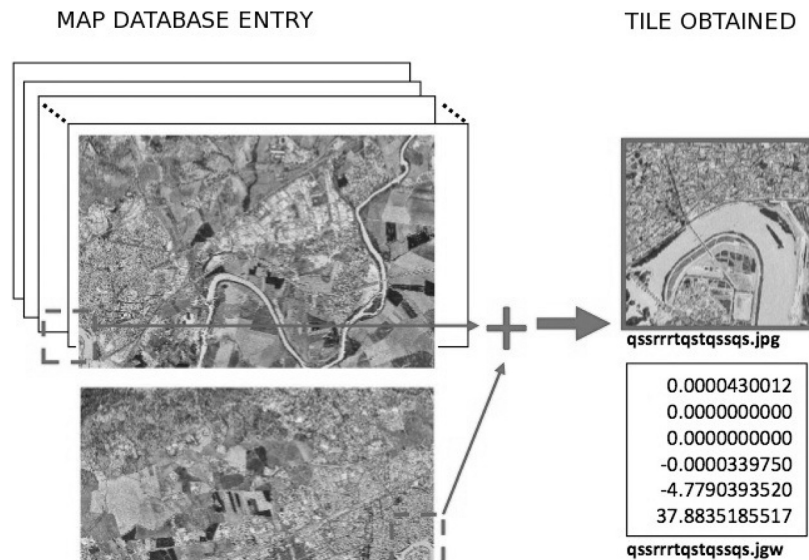


Figure 6. Splitting orthophoto to create tile.

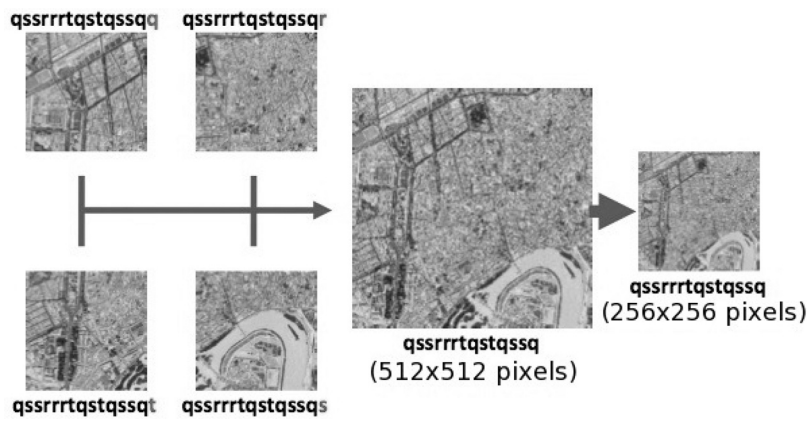


Figure 7. Joining and resizing four tiles to create the previous level tile.

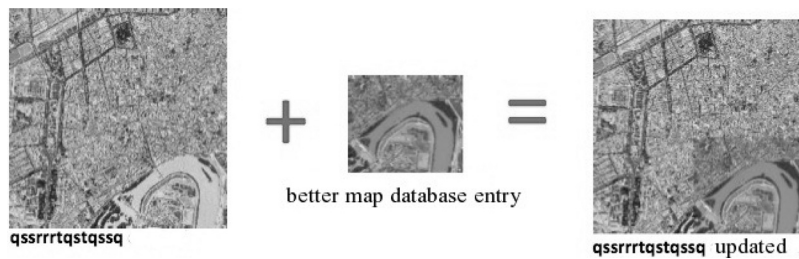


Figure 8. Updating tile given better map database entry.

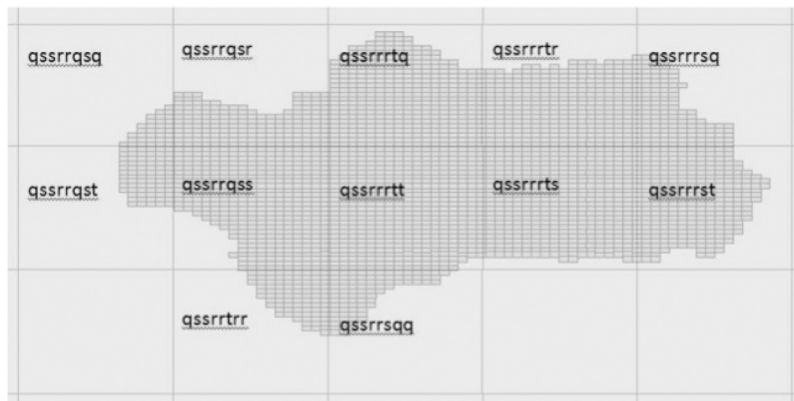


Figure 9. Tiles of level 8, which covers Andalusia.

The database entry consists of 2744 orthophotos with UTM and ED50, from which 136,593 jpg tiles were created with WGS84 and Mercator projection. Statistical methods were used to estimate map quality, with positive results, and the resulting map tiles have been included in Andalusia Envivo mapping services.¹⁶ The process was carried out by a computer with Intel Core 2, 1.86 GHz, 4 GB RAM, and took 3 days and 6 h.

Replacement

The highest level in the Andalusia pyramid of imagery tiles is 15. The main goal is to update tiles of two subpyramids (qssrrrtqsrqrqs and qssrrrtqsrqrtr, see Figure 10) that cover the area of Cordoba using a set of orthophotos with



Figure 10. qssrrrtqsrqrqs (left) and qssrrrtqsrqrtr (right) old tiles, to be updated.



Figure 11. Orthophoto in WGS84 Mercator.

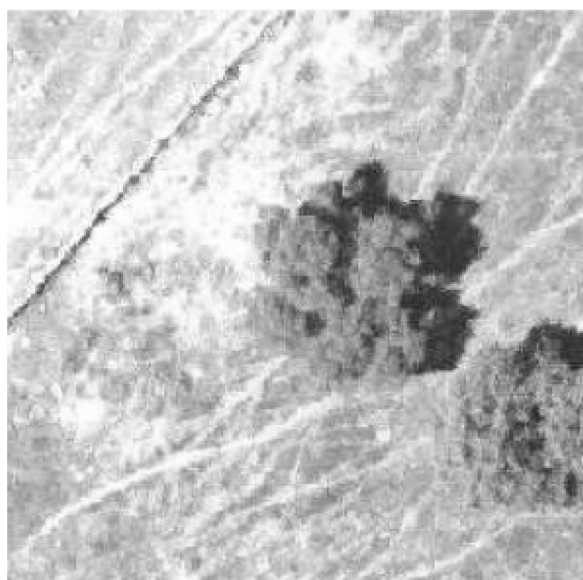


Figure 12. Tile "qssrrrtqsqrqrqrssrst."



Figure 13. From left to right: "qssrrrtqsqrqrqrqsq," "qssrrrtqsqrqrqrqsq," and "qssrrrtqsqrqrqrqsq."



Figure 14. Integration of the new and old mosaics.

Table I. Statistical variables for normal distribution surveys (m).

Function	Ex	Ey	RMSE
Min	-2.6201	-4.5524	0
Max	3.5802	4.1636	6.7834039
Range	6.2003	8.716	6.7834039
N	588	588	588
N_Sturges	10	10	10
Amplitude	0.63	0.88	0.68
N_Sturges*amplitude	6.3	8.8	6.8
N_Sturges*amplitude-range	0.0997	0.084	0.0165961
(N_Sturges*amplitude-range)/2	0.04985	0.042	0.0082981

Note: Min: Minimum aggregate function; Max: Maximum aggregate function; Range: Minimum interval containing the data; N: Number of geodetic stations; N_Sturges: Set of the number of class intervals using Sturges' rule; Amplitude: Range/N Sturges. Meter: (m) is the unit of length used in all tables.

Table II. Ex (m) for each class interval.

MinS	MaxS	MeanS	FrecS
-2.67	-2.04	-2.355	18
-2.04	-1.41	-1.725	28
-1.41	-0.78	-1.095	50
-0.78	-0.15	-0.465	89
-0.15	0.48	0.165	122
0.48	1.11	0.795	122
1.11	1.74	1.425	70
1.74	2.37	2.055	53
2.37	3	2.685	22
3	3.63	3.315	14

Table III. Ey (m) for each class interval.

MinS	MaxS	MeanS	FrecS
-4.6	-3.72	-4.16	13
-3.72	-2.84	-3.28	19
-2.84	-1.96	-2.4	36
-1.96	-1.08	-1.52	68
-1.08	-0.2	-0.64	106
-0.2	0.68	0.24	190
0.68	1.56	1.12	95
1.56	2.44	2	50
2.44	3.32	2.88	16
3.32	4.2	3.76	11

finer resolution of 0.15 m per pixel in UTM projection and ED50 coordinate system while adding five more levels to the pyramid.

First, the orthophotos needed to be converted into the WGS84 coordinate system with a Geographic Mercator

Table IV. RMSE (m) for each class interval.

MinS	MaxS	MeanS	FrecS
-0.01	0.67	0.33	78
0.67	1.35	1.01	155
1.35	2.03	1.69	151
2.03	2.71	2.37	85
2.71	3.39	3.05	45
3.39	4.07	3.73	35
4.07	4.75	4.41	17
4.75	5.43	5.09	15
5.43	6.11	5.77	13
6.11	6.79	6.45	6

Table V. Mean and standard deviation (m).

	Ex	Ey	RMSE
Mean	0.4215279	-0.057037	1.9313265
Standard deviation	1.2453233	1.536878	0.0828783

projection, yielding the result shown in Figure 11. Next, splitting algorithm is performed to create all tiles of level 20. Figure 12 shows an example of the highest level of detail that has been achieved in the new mosaic. Figure 13 shows new tiles with this higher resolution mosaic. The last step was the performing the joining algorithm to obtain updated lower levels of the pyramid. Figure 14 shows the integration of new and old mosaics.

GEOMETRIC ACCURACY OF THE QUADTREE STRUCTURE

The Federal Geographic Data Committee (FGDC) establishes and implements standards for data content, quality, and transfer.¹⁷ The FGDC defines a Data Usability Standard,

the National Standard for Spatial Data Accuracy¹⁸ (NSSDA). This is a statistical testing methodology for estimating the positional accuracy of points on maps and in digital geospatial data, with respect to georeferenced ground positions of higher accuracy.¹⁹ In this study, a method for evaluating the geometric accuracy of the orthophotos' quadtree structure based on the NSSDA standard is employed using geodetic stations as an independent source of higher accuracy to test the positional accuracy of maps. Geodetic control surveys are usually performed to establish a basic control network (framework). They are often employed when mapping control is required. In this study, 588 geodetic stations were used to estimate positional accuracy.

To estimate positional accuracy, root-mean-square error (RMSE), x-horizontal accuracy (Ex), and y-horizontal accuracy (Ey) are used. RMSE is the square root of squared differences between dataset coordinate values and horizontal coordinate values from a geodetic station for identical points. Ex is the difference between dataset x-horizontal coordinate values and x-horizontal coordinate values from a geodetic station for identical points. Ey is the difference between dataset y-horizontal coordinate values and y-horizontal coordinate values from a geodetic station for identical points.²⁰

Statistical Surveys

All collected data need to be condensed and simplified for better understanding and usefulness.²¹ Classification is the first stage in simplification. A total of ten class intervals were generated by applying Sturges' rule, see Table I. Amplitudes of 0.63, 0.88, and 0.68 are observed in the Ex, Ey, and RMSE class intervals, respectively. N Sturges* amplitude shows the new ranges computed for all class intervals, which exceed the initial ranges by 0.0997, 0.084, and 0.0165961, respectively. Therefore, the minimum and maximum need to be decremented and incremented by such quantities, which is applied to the first and last class intervals of Tables II-IV. Tables II-IV show values of Ex, Ey, and RMSE for

Table VI. Normal distribution table (m).

Ex		Ey		RMSE	
Normal Prob	Prob *N	Normal Prob	Prob *N	Normal Prob	Prob *N
0.0175194	10.301423	0.0070188	4.2393595	1.322×10^{-52}	7.934×10^{-50}
0.0466403	27.424521	0.0265094	16.011692	1.156×10^{-12}	6.937×10^{-10}
0.0966317	56.819432	0.0717146	43.315631	0.8830914	529.85485
0.1558244	91.624744	0.145009	87.585409	0.1169086	70.145151
0.1955859	115.00453	0.2101133	126.90842	0	0
0.1910908	112.36138	0.2212894	133.65882	0	0
0.145325	85.451116	0.1694037	102.31984	0	0
0.0860247	50.582528	0.0942555	56.930311	0	0
0.039633	23.30422	0.0381101	23.018489	0	0
0.0142101	8.3555568	0.0111948	6.7616496	0	0

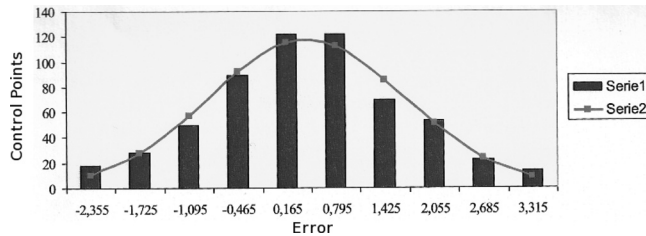


Figure 15. Bar diagrams and normal distribution of Ex.

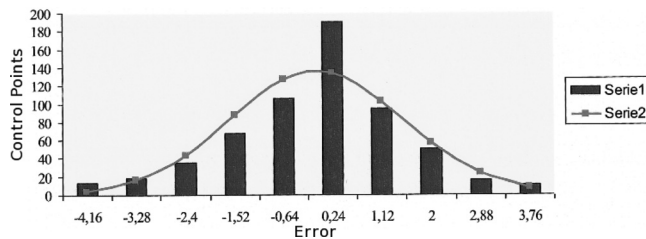


Figure 16. Bar diagrams and normal distribution of Ey.

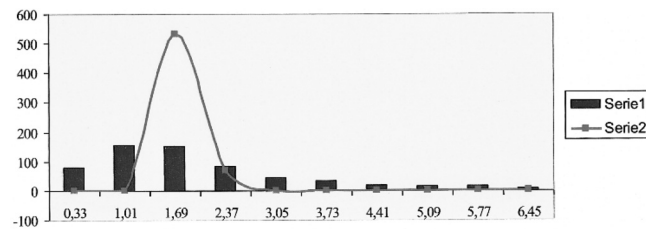


Figure 17. Bar diagrams and normal distribution of RMSE.

each class interval. MinS represents the minimum value of error for each interval, MaxS represents the maximum value of error for each interval, MeanS represents the mean value of error for each interval, and FrecS represents the number of control points, whose positional accuracy error is within the class interval. From data in Tables II–IV, mean and standard deviations were obtained, as shown in Table V, and normal distribution as shown in Table VI.

Normal plot analyses for each error variable Ex, Ey, and RMSE are represented in Figures 15–17, respectively. In these figures, the horizontal axis represents the mean error value of each class interval, and the vertical axis the number of control points whose positional accuracy error is within the class interval. The lines in the figures graph normal distribution of Prob*N in Table VI. The bar in the figures graph FrecS and MeanS in Tables I–IV, respectively. From these figures, it can be deduced that more than 90% of values for Ex, Ey, and RMSE are less than 2.5 m. All the results of this analysis were incorporated into the orthophoto geometric control metadata.

CONCLUSION

This article describes a systematic approach for interfacing with Google Maps' computing infrastructure, which enables the publication of large raster datasets within Google

Maps. The article also describes a methodology for evaluating the geometric accuracy of raster data. In this study, 1-m pixel resolution maps are used. Higher resolution maps can be used with the aim of creating a portal with better quality maps. A methodology for evaluating the geometric accuracy of the orthophotos' quadtree structure based on the NSSDA standard is presented. The method uses geodetic stations as an independent source of higher accuracy to test the positional accuracy of maps. It is shown that using 0.15 meter per pixel orthophotos, the proposed quadtree structure representation achieves an error of less than 2.5 m in more than 90% of control points.

REFERENCES

- A. Behrouz, *Introducción a la Ciencia de la Computación: De la Manipulación de Datos a la Teoría de la Computación* (Cengage Learning, México, 2003), p. 290.
- K. Sayood, *Introduction to Data Compression* (Morgan Kaufmann, San Francisco, CA, 2000), p. 2.
- D. Lelewer and D. Hirschberg, "Data Compression", *ACM Comput. Surv.* **19**, 291–296 (1987).
- R. Blake, *Sistemas Electrónicos de Comunicaciones* (Cengage Learning, Mexico, DF, 2004), p. 359.
- See <http://www.ermapper.com/> for Erdas, accessed June 13, 2011.
- ArcIMS et al, *Accelerating WebGIS with Image Web Server. Technical Overview and Performance Analysis* (Earth Resource Mapping, CA, 2002), p. 3. See also: www.resmap.com/pdf/acceleratingwebgis.pdf.
- See <http://www.lizardtech.com/> for LizardTech, accessed June 13, 2011.
- See <http://www.lanl.gov/> for Los Alamos National Laboratory, accessed June 13, 2011.
- D. Decker, *GIS Data Sources* (John Wiley & Sons, New York, 2000), p. 121.
- G. Aydin, A. Sayar, H. Gadgil, M. S. Aktas, G. C. Fox, S. Ko, H. Bulut, and M. E. Pierce, "Building and applying geographical information system grids", *Concurrency Comput.: Pract. Exper.* **20**, 1653–1695 (2008).
- P. Elissalde, "2D/3D web-mapping: Web visualisation coastal orthophotos", *Hydro Int.* **11**, 17–19 (2007).
- K. D. Sherwood, *Accessible GIS Visualizations* (University of British Columbia), <http://www.cs.ubc.ca/~tmm/courses/cpsc533c-05-fall/projects/ducky/report.pdf>, accessed June 13, 2011.
- J. Zheng, X. Chen, B. Ciepluch, A. C. Winstanley, P. Mooney, and R. Jacob, "Mobile routing services for small towns using cloudmade API and OpenStreetMap", *Proc. 14th Joint Int. Conf. on Theory, Data Handling and Modelling in GeoSpatial Information Science*, J. Shi, Q. Zhou, Y. Leung, and C. Zhou, Eds., (The Hong Kong Polytechnic University, 2010), pp. 149–154.
- D. Hernández, B. Felipe, F. J. González, *orto_pnoa_etr89_vs_ed50: programa para transformar la georeferenciación de imágenes tiff y geotiff de etrs89 a ed50 1.0* (Comisión de transición al Sistema de Referencia ETRS89, 2006).
- See http://www.gdal.org/gdal_utilities.html for Gdal Utilities, accessed June 24, 2011.
- Junta de Andalucía, Consejería de Turismo, Comercio y Deporte, "Andalucía En Vivo", *Revista de la Consejería de Turismo, Comercio y Deporte* **1**, 69 (2007).
- FGDC-STD-0007.1-1998, *Geospatial Positioning Accuracy Standards Part 1: Reporting Methodology* (Federal Geographic Data Committee, Washington, D.C., 1998), p. 1.
- FGDC-STD-007.3-1998, *Geospatial Positioning Accuracy Standards Part 3: National Standard for Spatial Data Accuracy* (Federal Geographic Data Committee, Washington, D.C., 1998), p. 1.
- FGDC-STD-007.2-1998, *Geospatial Positioning Accuracy Standards Part 2: Standards for Geodetic Networks* (Federal Geographic Data Committee, Washington, D.C., 1998), p. 1.
- J. Fallas, *Normas y Estándares Para Datos Geoespaciales*, Laboratorio de Teledetección y Sistemas de Información Geográfica (Universidad Nacional, Heredia, Costa Rica, 2002), pp. 5–6.
- R. Romero, *Integración de Ortofotografías Digitales en Plataformas Web de Consulta y Visualización* (Universidad de Córdoba, Córdoba, 2011), pp. 165–184.